NIU Journal of Social Sciences Copyright©2023
Nexus International University ISSN: *3007-1682*; 9(2): 51- 64

Enhancing Forest Landscape Spatial Data Modeling through Cloud-Based Approaches: A Case of Oluwa Forest Reserve, Ondo State Nigeria

N. E. ESSIEN, O.J. AIGBOKHAN
Forestry Research Institute of Nigeria.

O. OLABODE, R. O. AKINYEDE
Federal University of Technology, Akure, Nigeria

Abstract. The term "cloud computing" refers to Internet-based computing where virtual shared servers offer users software, infrastructure, platform, devices, and other resources on a pay-per-use basis. Remote sensing for the management of environmental resources can use cloud computing. Using cloud-based spatial data, this study will assess changes to the forest landscape in the Oluwa forest reserve. In this study, the reserve's existing and future forest cover is modelled utilising cloud data and cloud computing. This study shows how cloud computing may be used to detect different types of forest landscapes in Oluwa Forest Reserve based on projected future land cover patterns and simulated land cover utilising spatial data. The traditional approach to calculating forest cover is laborious and time-consuming. Using Google Earth and the cloud computing technology, it is possible to identify changes in forest cover more quickly and with less effort. According to the findings, forest land looked to have decreased between 1992 and 2022, with a larger rate of change between 2002 and 2012. The secondary forest increased with time as well, changing at a faster rate between 2002 and 2012 (approximately 6.5% growth) than between 2012 and 2022 (about 1.8% reduction). Between 1992 and 2022, non-forest land increased overall. Between 2002 and 2012, the non-forested area grew by 1.48%, while the 10-year period saw a 3.93% rise.

Keywords: Degradation, Cloud Computing, Modeling, Classification, Fragstats

1. Introduction

We depend on forests for a variety of goods and services, including wildlife habitat, hydrological functions, and carbon storage (FAO, 2009). Given the significant contributions that forests make to human well-being, it is important to know the status of our forests. Assessing the forests will show whether they are degrading and the likely causes of the degradation. In order to prevent additional deterioration and to restore and rehabilitate degraded forests, it is important to have accurate information on the condition of the forest and the degree of forest degradation. Uncontrolled tree-cutting and other human activities like farming and grazing are to blame for the rise in forest loss in the tropics, particularly in Africa (Isaac et al. 2018). These are elements that may increase human migration, energy costs, fire outbreaks, and other causes of forest loss (Yang 2001).

There aren't many landscapes left on the earth's surface today that haven't undergone a major change (Yang, 2001). Man's activities on the surface of the Earth have changed the terrain, and this change has had a significant impact on the surrounding environment (Yang, 2001). It is unavoidable to monitor the forest to track its status for proper and effective management to prevent forest mortality and improve the services of a forest (Soraya, 2013).

Data can be accessed through the cloud at any time and from any location. Recent advances in cloud computing have made it possible to track how the ecological landscape is evolving (Rakesh et al., 2014). Utilising time series cloud data, change detection measures changes in the landscape's land cover. These online data offer a comprehensive picture of the landscape type (Alexa et al., 2011). Indicating the variability of the ecological landscape, cloud data enable the evaluation of the forest landscape across a wide area (Alexa 2011). The availability of trustworthy cloud data collected by

satellite, with methodical processing and creative analytical tools, will aid in the timely and cost-effective monitoring and analysis of forest cover and landscape metrics of wide areas (Li and Yeh, 2004; Huth, and Cebula 2011).

For understanding and characterising landscape changes and their effects, landscape metrics—also known as spatial metrics—are essential (Li and Wu, 2004). Landscape metrics are indicators that can be used to pinpoint various facets of the organisation of a landscape through time and geography (Li and Wu 2004). In recent years, there has been a rise in the use of spatial metrics models for analysing the dynamics of our changing ecosystem's terrain. Dietzel et al. (2005) and Porter Bolland et al. (2007) are two examples. To evaluate the properties of the individual classes and the overall landscape, many metrics models have been applied (Li and Wu, 2004; Uuemaa et al., 2009).

These are crucial tools that ecologists use to visualise ecological processes and their outcomes and to better understand how they work (Bharath et al., 2012). The changes in landscape patterns at various scales are explained by multi-spatial satellite or cloud data (Saura et al. 2007). The classification of landscape diversity and variations within a forest estate is made easier by landscape metrics. Forest cover reduction and its effects on ecosystem processes that supply ecosystem services for human well-being are causing growing worry (Chapin et al., 2000; Millennium Ecosystem Assessment MEA, 2005). This area of study has seen a great deal of activity. Agbor et al. (2017) conducted research on Geospatial Technologies for Assessing Forest Losses in South-West Nigeria. Using bio-spectral models, the study calculated the amount of forest cover in South West Nigeria, including Oluwa Forest Reserve.

Growing concern is being expressed about the loss of forest cover and how it affects ecosystem processes that provide ecosystem services for human well-being (Chapin et al., 2000; Millennium Ecosystem Assessment MEA, 2005). There has been a lot of research in this field. Geospatial Technologies for Assessing Forest Losses in South-West Nigeria were the subject of research by Agbor et al. (2017). The study estimated the quantity of forest cover in South West Nigeria, including Oluwa Forest Reserve, using bio-spectral models.

Therefore, this study will use a more reliable model that can take into account all image pixels, creating a better categorization and analysis of the pattern of landscape change. Deforestation: Change Detection in Forest Cover Using Remote Sensing was the focus of Soraya Violini's (2013) research. This study looked at changes in forest cover but did not identify the causes of these changes or the fragmentation of the forest landscape, which is a crucial aspect of sustainable forest management. Toyinbo (2018) looked for signs of human activity in the Oluwa forest reserve. The project investigated the anthropogenic activities and affecting factors in Oluwa Forest Reserve.

In addition to looking at the causes of deforestation, this study will also look at landscape fragmentation. Flowers, B. et al. (2020) used data from three somewhat distinct years to undertake a study to comprehend the dynamics of habitat fragmentation of ecosystems. Area-weighted mean shape index (AWMSI), mean shape index (MSI), edge density (ED), mean patch size (MPS), number of patches (NUMP), and class area (CA) metrics were employed in the investigation. For the years 2001, 2011, and 2017, the measures were created. According to Mandal and Chatterjee's (2020) research, spatial change is the most effective way to enhance habitat quality while lowering the complexity of the habitat's design.

They made use of metrics including the fractal dimension (FD), shape index (SI), and perimeter area ratio (PAR). The Radhanagar Forest Range's habitat fragmentation was studied using these metrics. Forest degradation is a process of change that adversely affects a forest's features, resulting in a drop in the value and output of the forest's goods and services. Forests, according to the authors, are areas with a canopy cover of 10% or more and a surface area of up to 0.5 ha; they are defined by the presence of trees and the lack of any other major land use, and the trees must be able to grow to a minimum height of 5m. The law 26.331/07 of Minimum Standards for Environmental Protection of Native Forests in Argentina defines forest as natural forest ecosystems made up primarily of mature native tree species, with various species of flora and fauna associated, as well as the surrounding medium-soil, subsoil, atmosphere, climate, and water - forming an interdependent web with its characteristics and multiple functions.

Deforestation is defined by the Programme Forest Resources Assessment as the conversion of forests to other land uses or a reduction in their cover that is less than 10% of their total area (0.5 hectares). Deforestation is also described as the direct conversion of human-caused forest land to non-forest land by the United Nations Framework Convention on Climate Change (UNFCCC). A variety of

regionally specific economic, social, and political factors contribute to deforestation. According to Lowe et al. (1992), logging and the conversion of tropical forests to agricultural or grazing land are the main sources of deforestation. The Programme Forest Resources Assessment defines deforestation as the conversion of forests to other land uses or a reduction in the cover of forests that is less than 10% of the total area (0.5 hectares) of the forest. The United Nations Framework Convention on Climate Change (UNFCCC) defines deforestation as the direct conversion of human-caused forest land to non-forest land. Deforestation is influenced by several locally unique economic, social, and political factors. The main causes of deforestation, according to Lowe et al. (1992), are logging and the conversion of tropical forests into agricultural or grazing land. Using bio-spectral models, Agbor et al. (2017) calculated the amount of forest cover in South West, of Nigeria, including Oluwa Forest Reserve. The crew makes use of the Forest Canopy Index as a bio-spectral model. The data from the Advance Vegetation Density Index (AVD), Bare-soil Index (BI), and Forest Shadow Index (FSI) were combined to create the Forest Canopy Density Index (FCD). The density of the forest canopy is a crucial element in the Forest Canopy Density model for characterising the state of the forest. This model uses data from four indices (Slady, 2016) to simulate and analyse bio-spectral phenomena. A parametric statistical model was used by Agbor et al. (2012) and Soraya Violini (2013) to extract information about land cover from satellite images. The average rate of change, which measures how quickly one quantity is changing relative to another, was used in this procedure. In other words, it computes the difference between the change in one item and the change in the other item. In the Oluwa Forest Reserve, anthropogenic activities were identified by Toyinbo (2018), along with their effects on the forest cover. The study looked at the anthropogenic activities and affecting factors in Oluwa Forest Reserve. Using roads, water bodies, and built-up regions as independent factors, he regressed the forest as the dependent variable. Human disturbances also referred to as human development, were found to have the greatest influence. Uzoma and Moses (2014) investigated the use of GIS and remote sensing to detect land use change in the Omo Biosphere Reserve. Between 1987 and 2011, this study evaluated the trends of land use change in Nigeria's Omo Biosphere Reserve. The study employed Landsat TM imagery from 1987 and Landsat ETM+ imagery from 2011. They used ArcGIS 9.2 and Erdas Imagine 9.2 to determine and analyse changes in land use. They conducted the study using space-based data, which allowed them to evaluate the amount of forest cover in the past, which would have taken a long time using traditional surveying approaches.

Their main drawback was that they couldn't access some parts of the forest for accuracy evaluation. The findings showed that in 1987, areas occupied by farms, disturbed woods, communities, and rivers expanded while those occupied by natural forests, plantations, and highways shrank. Following disturbed woods (10917 hectares), towns (4262 hectares), and rivers (235 hectares), farmlands saw the largest area increase (19025 hectares) compared to 1987 estimates. Plantations (22699 hectares) experienced the greatest area decline, followed by natural forests (10803 hectares) and highways (937 hectares). Natural forests made up the majority of the reserve as of 1987, taking up 39.32% of it. Nevertheless, out of all land use types, disturbed forest today occupies the largest portion of the reserve (36.34%), followed by natural forest (32.05%), farms (14.78%), plantations (10.62%), settlements (4.11%), roads (1.22%), and rivers (0.87%). Due to excessive exploitation in the former and different conservation measures in the latter, the abundance of the natural forest cover drifted from the northeastern section of the reserve in 1987 to the northwestern part in 2011. It is anticipated that the data presented in this study will assist in making choices that will improve the reserve's sustainable management. Flowers, et al. (2020) used data from three somewhat distinct years to undertake a study to comprehend the dynamics of habitat fragmentation of ecosystems. Area-weighted mean shape index (AWMSI), mean shape index (MSI), edge density (ED), mean patch size (MPS), number of patches (NUMP), and class area (CA) are the metrics employed for the investigation. The measurements for 2001, 2011, and 2017 were created. In 10 years, agricultural land rose by 19.37%, but the NUMP of some habitats climbed by 284%. Additionally, the results revealed ED variation and a decline in total MPS, both of which pointed to significant fragmentation. According to Mandal and Chatterjee's (2020) research, spatial change is the most effective way to enhance habitat quality while lowering the complexity of the habitat's design. They made use of metrics including the fractal dimension (FD), shape index (SI), and perimeter area ratio (PAR). The Radhanagar Forest Range's habitat fragmentation was studied using these metrics. To determine the structural quality of the forest shape from the two maps, the study compared the index values. The comparison showed that the structural quality of the altered forest habitat was superior to that of the habitat quality of the current forest landscape.

2. Research Methodology

2.1 The Study Area

Oluwa Forest Reserve is positioned in the southwest of Nigeria, between latitudes 6º 40' and 7º59' N and longitudes 4º30' and 4º55' E (Figure 1). The region, which is 859 km^2 in size, is located on southern Ondo State's borders. The terrain's approximate height above sea level is 133 metres. It is a part of the Omo-Oluwa-Shasha Forest complex, a collection of forest reserves in southwest Nigeria. Despite being divided from the Omo and Shasha reserves (which are still connected as of 2011), the three reserves contain some of the last intact woodlands in the area. Despite the physiological differences between them, logging, hunting, and agriculture are threats to them (Oke, 2013). The average yearly rainfall in the area is about 2050 millimetres, while the average monthly temperature is roughly 27 °C. The natural vegetation, which was previously lowland tropical rainforest (wet evergreen type), has been reduced to secondary forest, thickets, and various degrees of fallow regrowth or annual and perennial crops, except some portions of the forest reserves. The reserve is surrounded by a region of wet mixed semi-evergreen rainforest. While Nauclea diderrichii and Terminalia superba are more common in the reserve's moist central portions, Sterculia rhinopetala and other common species are more common in the reserve's drier northern regions (Ola-Adams, 1999). In the wet forests in the south, which are situated on sandy marshy soils, lophira and trees from the Meliaceae family are also widely distributed. Over the course of over a century of continuous human activity, mostly farming and logging, the vegetation pattern of Oluwa has undergone significant change. There are also natural woodlands that have been disturbed to varied degrees.

Tropical ferruginous soils predominate (Hall, 1977). They fall into the upper classification category's Ferric Luvisols type (Chijioke, 1980). The reserve contains a variety of soil types, however they all fall within the category of tertiary sediments (Ola-Adams, 1999). The reserve is located on crystalline rocks of the undifferentiated foundation complex, which are overlain by Eocene deposits of sand, clay, and gravel in the southern portions (Isichei et al 1995). The Reserve's lowest points are in the south, and the topography is undulating with a maximum elevation of 150 m above sea level in the west. The Reserve has a tropical wet-and-dry climate, which has two rainfall peaks that are separated by a somewhat dry phase that typically occurs in the month of August. The mean relative humidity is 80%, and the mean annual rainfall is approximately 1750 mm. The average daily temperature was determined to be 26.4 °C, which is 0.6 °C higher than Evans's (1939)'s average daily temperature of 25.80 °C. Typically, between 8 and 10 hours of sunshine per day are experienced throughout the wet season.

The US Geological Survey (USGS) website was mined for cloud data from Landsat satellite images taken in 1992, 2002, 2012, and 2022 to achieve the research objectives. Located on row 55 and Landsat path 190 is the research area. The images have pixel sizes of 30x30m (Chander, 2003). All of the images were taken during the same period (the dry season). The Level 1 Terrain Corrected (L1T) product of the gathered Landsat data was pre-georeferenced to the UTM zone 31 North projection using the WGS-84 datum. The images in this experiment received preprocessing.

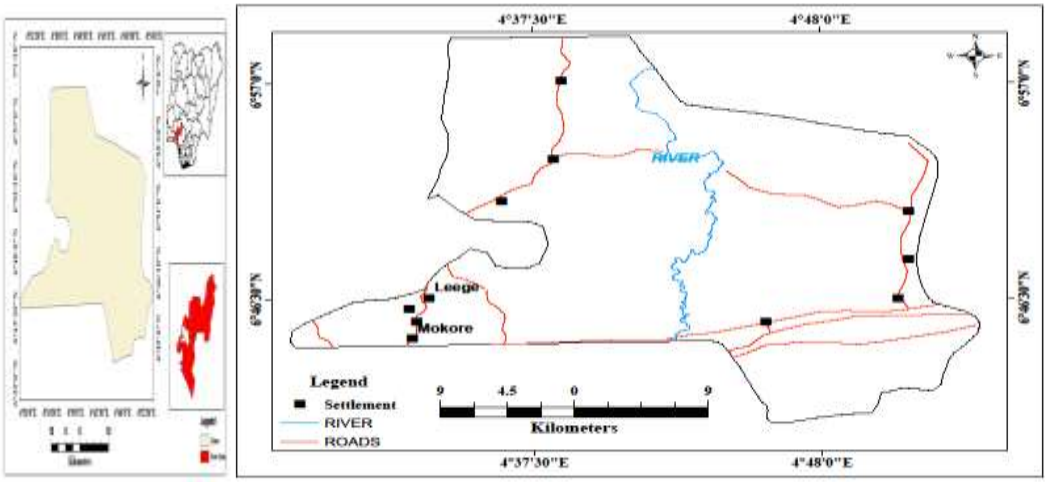

Fig. 1: *The study area.*

2.2 Data Set

To accomplish the research goals, cloud data from Landsat satellite photos taken in 1992, 2002, 2012, and 2022 were mined from the US Geological Survey (USGS) website. The research region is situated on row 55 and Landsat path 190. The photos have 30x30m pixel sizes (Chander, 2003). The same season (dry season) was used to capture all of the photographs. WGS-84 datum was used to pre-georeference the collected Landsat data (Level 1 Terrain Corrected (L1T) product) to UTM zone 31 North projection. In this investigation, the pictures underwent preprocessing. The details of the Landsat TM, ETM+, and OLI pictures are shown in Table 1.

Table 1: Research Materials to Use

Satellite Sensor	Spatial resolution	Acquisition years	Path	Row
Landsat 5, 7 & 8	30m x 30m	1992 2002.2012, and 2022	190	55
Asterdem	30m interval	2018	-	-

The cloud data (Landsat image) were obtained via Google Earth Engine as shown in Figure 2. This figure shows the black and white Landsat data mined from the Google archive. The black and
white images were enhanced by creating their composites as shown in Figure 3.

Figure 2.: *Black and white Landsat image*

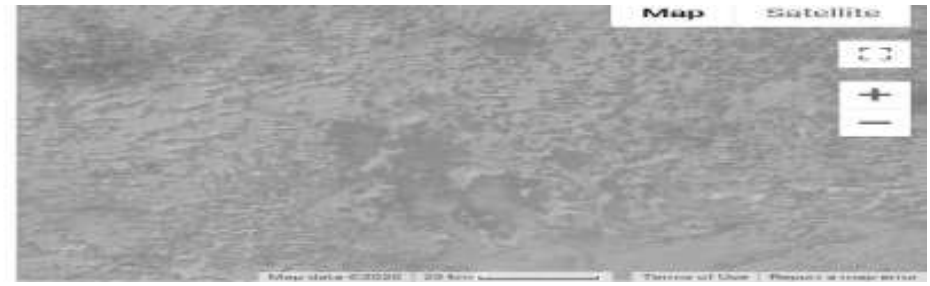

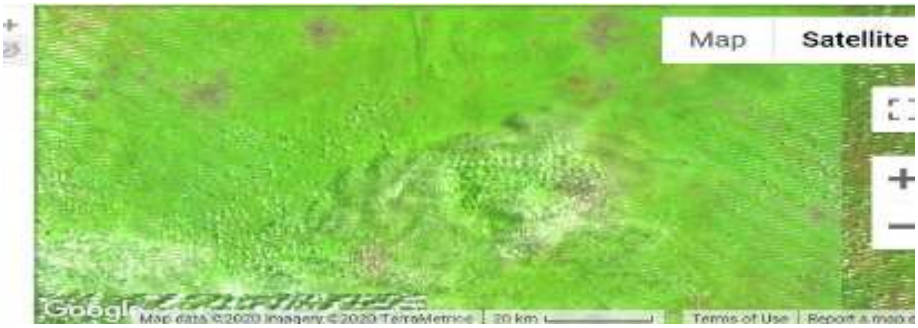

Figure 3: Composite image on Google Earth Engine
The black and white images were enhanced by creating their composites as shown in Figure 3.

2.3 Data Preprocessing

According to Giannini et al. (2015), each pixel in raw remote sensing data contains a digital number value that corresponds to a raw measure needed by the sensor. Images must be transformed from digital numbers to physical quantities, such as radiance and brightness temperature, to extract quantitative information from them. The previously calibrated photos must be adjusted for atmospheric impacts. The radiometric signal may be significantly distorted when the atmosphere is present. Using equation 1 (Giannini et al., 2015), the pictures utilized in this investigation were first converted to Top of Atmosphere (TOA) radiance.

$$\mathrm{TOAr} = \left(\frac{(L_{MAX\lambda} - L_{MIN\lambda})}{Q_{CAL}}\right) Q_{CAL} + L_{MIN\boldsymbol{\lambda}} \quad (1)$$

Where;
$L\lambda$ the radiance at the aperture [W/(m^2 sr µm)]
Q_{CAL} is the Quantized calibrated pixel value [DN]

$L_{MIN}\ \lambda$ is the Spectral at-sensor radiance that is scaled to Q_{CAL}MIN [W/ (m^2 sr µm)]
$L_{MAX}\ \lambda$ is the Spectral at-sensor radiance that is scaled to Q_{CAL}MAX [W/ (m^2 sr µm)]. The above expression does not consider the atmospheric effects, therefore there is need to convert images from radiance to reflectance measures, using equation 2 (Gyanesh *et al*, 2009).

$$\rho\lambda = \frac{\pi.TOAr.d^2}{E_{SUN}\lambda.Cos\theta_{sz}}$$

(2)
Where;
$\rho\lambda\ is\ the$planetary TOA reflectance (unitless)
$\pi\ is$ approximately159
$d^2\ is\ the$ Earth-Sun distance (Astronomical unit)
$E_{SUN}\lambda\ is\ the$ mean exoatmospheric solar irradiance [w/ (m^2 sr µm)].
Θ_{SZ} is the solar zenith angle (degree). The cosine of this angle is equal to the sine of the sun elevation θ_{SE}. That is, $\theta_{SZ} = 90 - \theta_{SE}$.

2.4 Data Collection

The geographic coordinates of the observation sites from the GPS reading will be recorded, and the positions will be indicated on the satellite photos, and the GCPs will be located in the field using a GPS, topographic maps, and Landsat satellite images. The number, accuracy, and distribution of the GCPs will be taken into account when gathering the data, and a small sample of points (GPS points) representing a particular land use or cover type will be chosen at random in the field. With the GPS device, this will be done throughout the study region, and 100 sample sites will be chosen. A similar amount of GPS points (100 sample points) will be utilized to evaluate the classification accuracy.

Image Classification
To classify the images, a modified version of the Anderson scheme of land use/cover classification was adopted and the categories include:
(a) Forest area
(b) Grassland
(c) Bare surface area

Cloud data (Image geoprocessing is the computer-aided alteration and analysis of images. (2008) Lillesand et al. Digital image processing is based on the principle that an image should be sent to a computer that is programmed to insert it into an equation or set of equations and then save the results of the computation for each pixel of the image. The outcomes result in a brand-new digital image that can be exhibited or captured in pictorial format, as well as further altered by other programmes. (2008) Lillesand et al.
In each band of imaging, the intersection of each row i and each column j contains the picture elements (pixels) that make up a digital cloud or satellite data (pictures) (Jensen, 1996). The Digital Number (DN) or Brightness Value (BV) assigned to each pixel serves as a representation of the average brightness of a very tiny area inside the image (Jensen, 1996). A smaller value denotes an area with low average radiation, while a greater number denotes an area with high radiant characteristics. In 2000, Jensen. Figure 3 shows a black-and-white, 30-by-30-pixel image of the study area. The main goal of image classification is to automatically assign land cover classes or themes to all of the pixels in an image. The spectral pattern found in the data for each pixel is employed as a numerical basis for classification when multispectral data are used to do the classification. According to their innate spectral reflectance and remittance characteristics, many feature types exhibit various combinations of DNs (Lillesand et al., 2008). The unsupervised and supervised techniques of classification are the two basic approaches used in classical methods. The image analyst oversees the pixel classification process in the supervised approach to classification, which was used for this work, by providing the computer programme with numerical descriptors of the different land cover classes present at the study area. This was done by creating a numerical interpretation key that defines the spectral properties for each feature type of interest using representative sample sites of recognized cover categories, often known as training areas or training sites (Lillesand et al., 2008).

2.5 Assessment of Forest Landscape Changes and Spatial Distribution

The images were divided into three categories: bare land, grassland, and forest land to evaluate the spatiotemporal pattern of forest cover. The land use/cover changes between 1992 and 2022 were calculated using a simple percentage (equation 3.3) and a dynamic weight model (equations 3 and 4), both of which used data from cross-classification (Liu et al., 2011), to establish the rate of change.

$$\text{Cross classification} = \frac{S_{i-j}}{t} \times 100 \quad .$$

(3)

$$s = \sum_{IJ}^{N} \left(\frac{\Delta s_{I-J}}{s_I}\right) \times \frac{1}{T} \times 100$$

(4)
Where;
S_I is the area of land type i in the beginning of the period,

ΔS_{I-J} is the total area of land cover type *I* converted into other types
T is the study period; and
S is the land cover dynamic
Some spatial measures have been chosen to measure and monitor the landscape fragmentation, land use complexity, proximity, and diversity (McGarigal, et al. 2008) to evaluate changes to the forest landscape using metric models. To understand the local landscape dynamics, these spatial metrics will be produced using FRAGSTAT interfaced with ArcGIS. Class Diversity Index, Class Evenness Index, Proximity Index, Shape Index, and Number of Patches are among the chosen criteria. Ecologists have measured the composition of the landscape using these indexes.

Table 2: Selected Spatial Metrics

S/N	Indicators	Formula	Range	Significance/ Description
1	Mean patch size (MPS)	$MPS = \frac{\sum_{i=1}^{n} a_i}{n_i} \frac{1}{10{,}000}$	MPS>0, without limit	MPS is widely used to describe landscape structure. MPS is a measure of subdivision of the class or landscape.
2	Class diversity index	$the\ C_d = -\ln \sum_{a=1}^{n} P_a^2$	$C_d \geq 0$ C_d = 0 when the area contains only 1 fragment and it means no diversity.	This measures the relative patch diversity of class a. This diversity index has been used by ecologists to measure landscape composition.
3	Proximity Index (MPI):	$\boldsymbol{the\ p_{rox} = \sum_{s=1}^{n} \frac{w_{abs}}{d^2_{abs}}}$	$Prox \geq 0$.	This is the sum of patch area (m^2) divided by the nearest edge-to-edge distance squared (m^2) between the patch and the focal patch of all patches of the corresponding patch type whose edges are within a specified distance (m) of the focal patch
4	Number of Patches	$N_p = n_a$	$NP \geq 0$, without limit. NP = 1 when the landscape contains only 1 patch.	A number of patches of a particular patch type is a simple measure of the extent of subdivision or fragmentation of the patch type.
5	Class Evenness Index	$C_e = -\ln \sum_{a=1}^{n} P_a^2 \div \ln n$	$0 \leq C_e \leq 1$	This measures the patch distribution and abundance of class a

Turner, 1990a, Rajesh et al, 2009, and Bharath et al, 2012

2.6 Cloud Technology

A cloud-based image processing solution that makes use of the Google Earth Engine's computer power is known as cloud technology. It supports Earth Observation analysis with a variety of features. This study will concentrate on applying the Change Detection approach to carry out a direct (supervised) change detection. Using a prebuilt mosaics module, the guided change detection system enables users to categorize change between two dates. Additionally, training data will be gathered via Collect Earth Online. Therefore, using the training data that will be put into Google Fusion Tables, the change detection analysis will try to pinpoint changes that occurred in the Oluwa forest reserve between 1992 and 2022. Using the distinctive Id that will be transferred to the clipboard, this table is connected to the cloud driver and the change detection module. The change detection analysis classification will now be handled by cloud technology, and the output results will be displayed on the screen. On the servers hosting the Google Earth Engine, this analysis will be done. Therefore, using the training data that will be put into Google Fusion Tables, the change detection analysis will try to pinpoint changes that occurred in the Oluwa forest reserve between 1992 and 2022. Using the distinctive Id that will be transferred to the clipboard, this table is connected to the cloud driver and the change detection module. The change detection analysis classification will now be handled by cloud technology, and the output results will be displayed on the screen. On the server for the Google Earth Engine, this analysis will be performed.

2.7 Forecast of Landscape Changes Using Cellular Automata Markov.

To represent continuous data over space, a raster data model in GIS Cellular Automata Markov (CA Markov-based) will be utilised. The area will be divided into pixels or grid cells by the model. The measured attribute values in a matrix will be entered into each grid cell, and the cell values will be recorded in rows and columns. For instance, CA-Markov models depict a forest with a lattice of cells, where each cell can exist in one of a limited number of states. Future patterns will be set by transition rules that specify how cells should behave across time, with time progressing as a series of distinct steps (Kampanart et al., 2005). As a result of the conditions at each cell and its neighbouring cells at

each time step, for instance, a cell may change from a forest region to a built-up area. Each land is represented by a pixel value from the raster data model in the categorised photos and the CA-Markov simulated images. The Markov model is calculated thus using equation 5.

$$S(t, t+1) = Pij \times S(t) \quad (5)$$

Using land use and cover change data derived from satellite images, this study will also establish the validity of the Markov process for describing and projecting land use and cover dynamics. The Markov chain has *n* states. The data vector is a column vector whose *ith* component represents the probability that the system is in the *ith* state at that time. It is important to note that the sum of the entries of a state vector is 1. For example, vectors X_0 and X_1 in the above example are state vectors. If p_{ij} is the probability of movement (transition) from one state j to state i, then the matrix

$$T = [p_{ij}] \quad (6)$$

is called the transition matrix as seen in equation 6 of the Markov chain (Kampanart *et al,* 2005 Takayama *et al*, 1997*).* A transition probability matrix and a transition regions matrix are the outputs of the CA-Markov analysis that was used to assess two images of land cover. The likelihood that each land cover category will change from each other is explained by the transition probability matrix. The number of pixels that are anticipated to change from one land cover type to another during the specified number of time units is represented by the transition areas matrix. A four-state Markov probability matrix has been created as a result of this. To project, the study will use cellular automata markov change prediction module in Idrisi software (Agbor *et al*, 2012 and Bangladesh *et al*, 2013). This was also manually calculated using a matrix model (equation 3.9). Both methods utilized the transition probability matrix generated from image cross classification as seen in equation 7.

$$A = \begin{pmatrix} x_{a_{11}} & x_{a_{12}} & x_{a_{13}} \\ x_{a_{22}} & x_{a_{22}} & x_{a_{23}} \\ x_{a_{31}} & x_{a_{32}} & x_{a_{33}} \end{pmatrix} B = \begin{pmatrix} x_{b_1} \\ x_{b_2} \\ x_{b_3} \end{pmatrix} C = \begin{pmatrix} x_{c_1} \\ x_{c_2} \\ x_{c_3} \end{pmatrix} \quad (7)$$

Where

A is the array of probability values of land cover types conversion.

B is the percentag of land cover types for the base year.

C is ththe projectedatrix.

The product of *A* and *B* matrices produced the forecast values matrix *C* for each land cover type. The output of projection by calculation was compared with the output of the projection module in Idrisi software.

The overall accuracy for the module is calculated as seen in equations 8, 9, 10 and 11.

$$Y = \frac{\sum_{i=1}^{n} X_i}{N} \times 100 \quad (8)$$

Producer's Acc $= \frac{w}{w+x}$ (9)

$\sum_{j=1}$

User's Accuracy $= \frac{y}{y+z}$ (10)

Where

w = number of times a classification agreed with the observed value,

x = number of times a point was wrongly classified,

y = number of times a point was correctly classified, and

z = number of times a point was not classified as 'a' when it was not observed to be 'a'h8vgv

Kappa's coefficient measures perfect agreement between prediction and reality or classification results and real observation, as is the case in this study. It was computed as:

$$K = \frac{N \sum_{ij=1}^{r} X_{ij} - \sum_{ij=1}^{r} (X_{ij} + X_{x+1})}{r} \quad (11)$$

Where r = numb $\mathcal{N}^2$ s and $\sum (X_{ij} X_{x+1})$ matrix,

N = total number of observations $_{ij-1}$

xij = observations in the ith row a olumn,

x+i = marginal total of the ith row, and

x+j = marginal total of the jth column.

3. Results and Discussion

3.1 Data Analysis

The outcomes are shown in the form of charts, maps, and tables. They include the static, changes in landscape types, significant variables that lead to change in landscape types in the study area and the future pattern of landscape changes in the area.

Landscape changes and their spatial distribution using metrics models. The static land cover distribution for each study year as derived from the images (Figures. 4-7) is presented in Table 3.

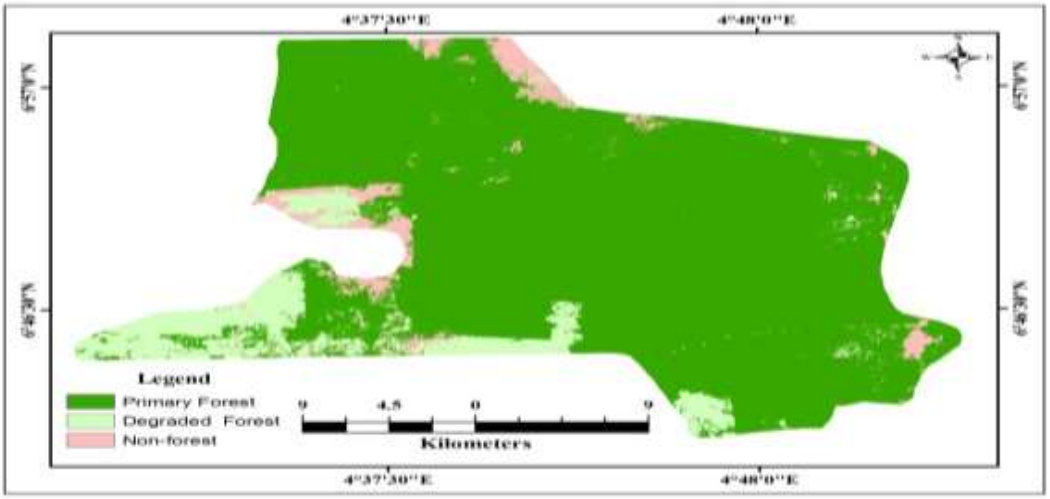

Figure 4: *Land cover map of Oluwa forest reserve in 1992*

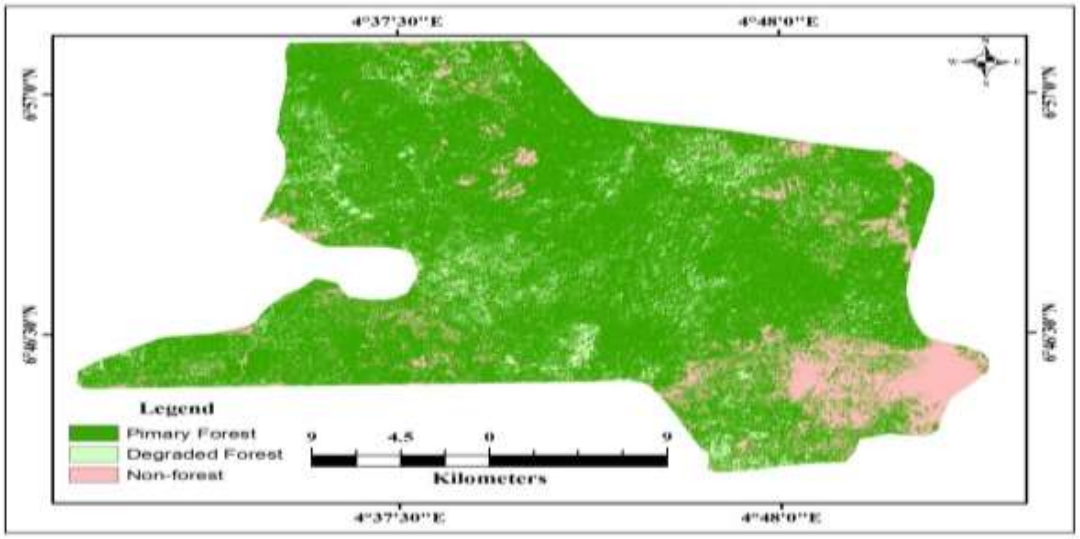

Figure 5: *Land cover map of Oluwa forest reserve in 2002*

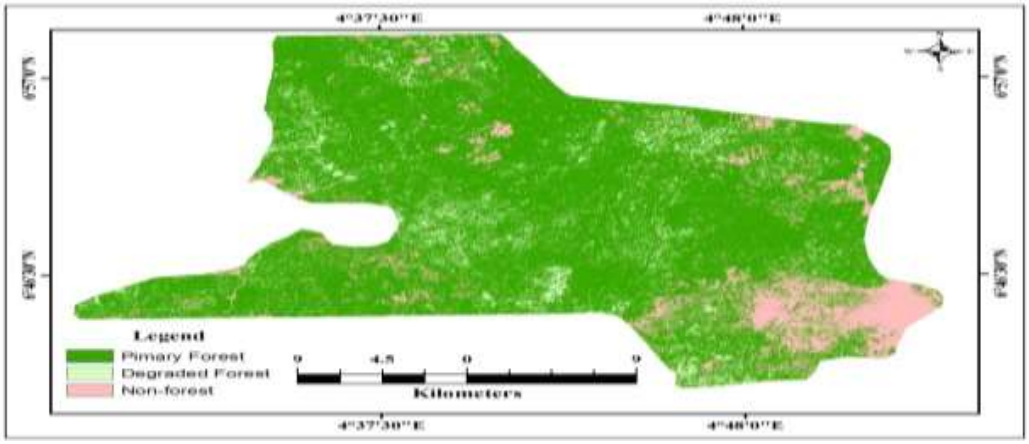

Figure 6: *Land cover map of Oluwa forest reserve in 2012*

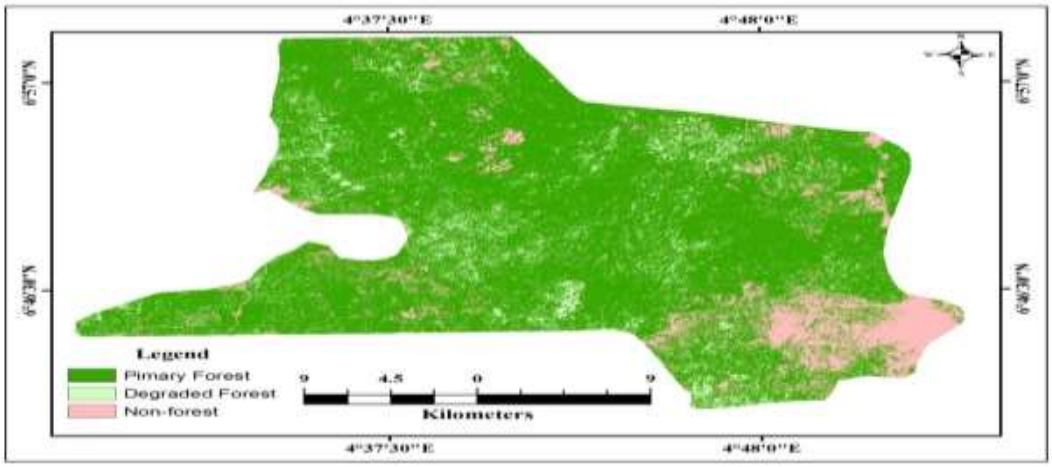

Figure7: *Land cover map of Oluwa forest reserve in 2022*

Land Cover maps for 2002, 2012, and 2022 are displayed in Figures 4.1–4.4, respectively. The images depict the land cover of the study region in 1992, 2002, 2012, and 2022 as shown on a land cover map of the Oluwa Forest Reserve for those years. The primary forest is shown in green, the degraded forest is shown in light green, and the non-forested region is shown in pink. The reserve's northern and western regions were mostly where the non-forest was located. Mostly primary forest made up the centre portion of the forest, while degraded forest made up the southern portion.

The continual loss of the area's natural forests and marshes over 27 years was shown to be caused by encroachment and illicit logging. Additionally, it appears that politics may have contributed to the demise of the forest. For instance, between 2002 and 2012, woodlands increased, and water bodies/swamps appeared to be largely steady. The statistics on the distribution of land cover are presented in Table 3.

Table 3: The Land cover spatial distribution statistics

Land cover categories	1992		2002		2012		2022	
	Area (Km)	Area %	Area (Km)	Area %	Area (Km)	Area %	Area (Km)	Area %
Primary forest	732.000	85.131	693.083	80.604	624.090	72.579	600.60	69.85
Degraded forest	85.808	9.979	90.969	10.579	147.250	17.126	132.07	15.36
Non-forest	42.052	4.890	75.808	8.817	88.520	10.295	127.19	14.79
Total	859.860	100.000	859.860	100.000	895.860	100.000	859.86	100

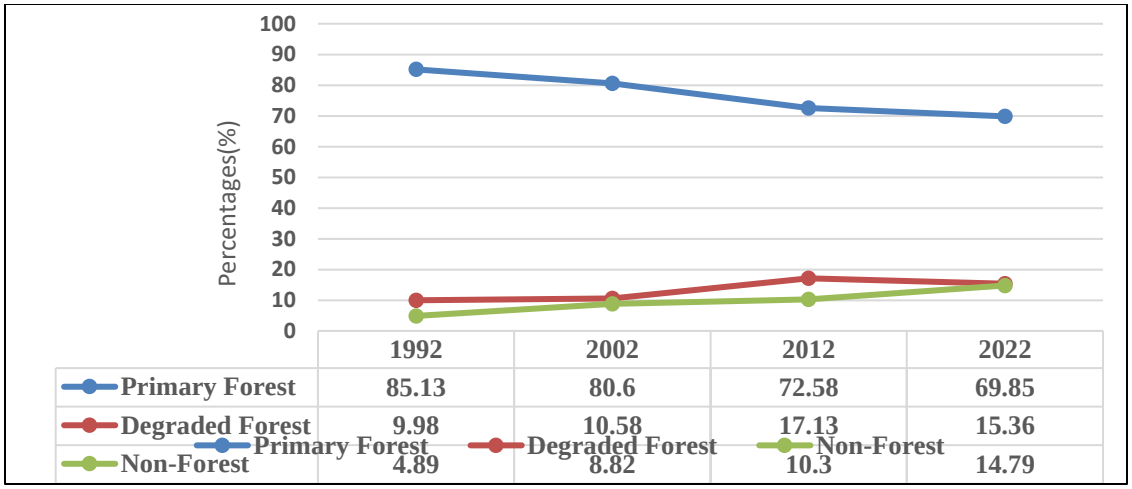

Line graph of land cover from 1992 to 2022

According to Table 3, forest land looked to have decreased between 1992 and 2022, with a higher rate of change occurring between 2002 and 2022. The secondary forest increased with time as well, changing at a faster rate between 2002 and 2012 (approximately 6.5% growth) than between 2012 and 2022 (about 1.8% reduction). Between 1988 and 2018, there was an overall rise in the area that wasn't forests. Between 2002 and 2012, the non-forested area grew by 1.48%, while the 10-year period saw a 3.93% rise. The alterations seen in the forest areas between 1992 and 2012 do not show this. This demonstrates that the most recent years saw the greatest loss of forest due to human activity. This is in line with research by Meshach et al. (2020) on a forest reserve, which revealed that the reserve underwent significant alteration over 27 years. Forest patches became dispersed as a result of the alterations. This study's finding is supported by additional studies by Adeyemi and Oyeleye from 2021. According to Oates et al. (2014), who conducted a similar study, the decline in natural forests was primarily caused by population growth, rapid urbanisation, and a lack of oversight from concerned forest management authorities. This conclusion is in line with Yu and Suganda (2012), who noted that vegetation cover decreases when factors like population growth are present. Additionally, there were indications of illicit wood extractions, which had a significant impact on the period's forest losses (Meshach et al. (2020, Adeyemi and Oyeleye 2021). The outcome of land use and land cover is consistent with (Kumar and Briti 2022) who proposed that there is a direct relationship between human activities and the depletion of the forest. The majority of subsistence farming methods indicate a slow but persistent degradation of the forest. The reserve contains several eroded sections. At the edges of the forest, the effects of deforestation are extremely noticeable. According to Meshach et al (2020), the change is currently caused by illegal and unrestrained logging that has devastated most of the forest, leaving it open to farmers for agricultural uses.

3.2 Image Classification Accuracy Assessment.

The producer's accuracy (Pa), user's accuracy (Ua), kappa statistics, and overall accuracy are all included in the accuracy statistics (Table 4). The Kappa Coefficient was used to calculate the accuracy values, as stated. The overall statistical picture indicates that the land cover analysis image classification was accurate.

Table 4: Error Matrix for years 1992, 2002, 2012, and 2022

Class Name	1992 $Pa, Ua.$	2002 $Pa, Ua.$	2012 $Pa, Ua.$	2022 $Pa, Ua.$
Primary forest	64, 78	50, 72.73	75.86, 78.60	78.86, 78.60
Secondary forest	51, 65	58.82, 78.13	66, 83.12	77, 83.12
Non-forest	96, 92	97.99, 90.15	97.79, 90.78	87.79, 90.78
KappaStatistics (k)	0.60	0.70	0.78	0.80
Overall accuracy	88.75%	87.75	88.50	89

$Pa, = producer's\ accuracy, Ua = users' accuracy$.

3.3 Forest Landscape Characterization

For ecologists and decision-makers, the negative effects of landscape fragmentation and heterogeneity development are a constant concern. The decrease in the overall area covered by forest trees is one of the main issues caused by this occurrence. It is clear from Table 4 that the number of patches (NumP) rose between 2002 and 2012 before falling in 2022. This suggests that recent years have seen a decrease in the fragmentation of the forest cover. The variations in NumP are reflected in the mean patch size (MPS), which climbed in 2022 after decreasing between 1992 and 2012.

This suggests that while the forest reserve had some forest Patches cleared, it eventually became a smaller single unit in 2022. The estimated Mean Proximity Index (MPI) for forest land, which grew with time, also shows that the forest cover was declining. The fact that class variety has increased over time, peaking in 2008, also suggests that class segments have grown from 1992 to 2012. The reduction of forest area over the years, as seen in Table 5, led one to the conclusion that reduced parts were given up to other land cover categories.

The growth of agricultural and grassland areas primarily came at the expense of plantation and natural forests. Due to cultivation and the rising demand for wood resources, plantations and natural forests underwent deforestation, degradation, and exploitation as a result of the development of agricultural land and grassland. Because the majority of the soils in the Reserve are nutrient-rich and excellent for agricultural production, the rich soils are more vulnerable to agricultural growth (Meshach et al. 2020).

Table 5: Metric statistics

	1992				
Land cover	MPS	SDI	SEI	NUMP	MPI
Primary forest	46.07	0.51	0.47	1589	201633.6
Degraded forest	6.67	-	-	1287	5902.4
Non-forest	1.47	-	-	2865	483.92
	2002				
	MPS	SDI	SEI	NUMP	MPI
Primary forest	26.74	0.68	0.62	2508	353928.7
Degraded forest	0.41	-	-	20073	44.39
Non-forest	0.84	-	-	12753	1651.34
	2012				
	MPS	SDI	SEI	NUMP	MPI
Primary forest	19.06	0.77	0.7	3274	392932.5
Degraded forest	2.14	-	-	6885	2667.26
Non-forest	3.76	-	-	2357	5098.75
	2022				
	MPS	SDI	SEI	NUMP	MPI
Primary forest	339.79	0.76	0.69	185	432565.6
Degraded forest	37.05	-	-	397	6630.03
Non-forest	30.95	-	-	272	5321.71

4. Conclusion and Recommendations

Plantation and natural forests were mostly lost to the expansion of agricultural and grassland areas. Plantations and natural forests endured destruction, degradation, and exploitation due to cultivation and the increasing need for wood resources as a result of the creation of agricultural land and grassland. Rich soils are more susceptible to agricultural growth because the majority of the Reserve's soils are nutrient-rich and ideal for agricultural output (Meshach et al. 2020). To assure the preservation of the natural forest, for instance, fifty seedlings of the same species as those that were cut down might be planted, but this raises the possibility of losing further indigenous species. During picture analysis, we found that monoculture plantations already resembled the natural forest, which will soon reduce species variety and native species. The final LULC map of 2022 in Figure 7 shows the visible land use changes that occurred in the Oluwa Forest Reserve between 1992, 2002, 2012, and 2022 as well as letting us know how the forest reserve is now doing. This graphic emphasises the vegetation changes and evaluates the change's severity on a qualitative level. This method made it evident where Oluwa Forest Reserve alterations have occurred.

References

Adeyemi, A.A. & Adeleke, S.O. 2020. Assessment of Land-cover Changes and Carbon Sequestration Potentials of Trees Species in J4 Section of Omo Forest Reserve, Ogun State, Nigeria. Ife Journal of Science 22(1): 137-152.

Adeyemi, A. A and Oyeleye, H.A. (2021). Evaluation Of Land-Use And Land-Cover Changes Cum Forestdegradation in Shasha Forest Reserve, Osun State, Nigeria Using Remote Sensing

Adeyemi, A.A. & Ibrahim, T.M. 2020. Spatiotemporal analysis of land-use and land-cover changes in Kainji Lake National Park, Nigeria. Forestist 70(2): 105-115

Agbor, C.F., Aigbokhan, O. J., Osudiala, C.S., and Malizu, L. (2012). Land Use Land Cover Change Prediction of Ibadan Metropolis. *Journal of Forestry Research and Management.* Vol.9, 1-13; 2012. ISSN: 0189-8418

Agbor, C. F., Pelemo O. J., Aigbokhan, O. J., Osudiala, C. S. and Alagbe, J. (2017). Forest Loss Assessment in South-West Nigeria Using Geospatial Technologies. *International Journal of Applied*

Research and Technology ISSN 2277-0585

Akinnifesi, F.K. and Akinsanmi, F.A. (1995) Linear Equations for Estimating the Merchantable Wood Volume of Gmelina arborea in Southwest Nigeria. *Journal of Tropical Forest Science*, 7, 391-397.

Alexa (2011). Exploring user interactions with Amazon Alexa: *Journal of Librarianship and Information Science* 51 (4).

Chander, P., (2003). The Core and Coalition Formation, CORE Discussion Paper 2003, 140.Chijioke (1980). Impact on soils of fast-growing species in low land humid tropics. FAO Forestry Paper (FAO: Rome).

Chapin III, F. S., Zavaleta, E.S., Eviner, V.T., Naylor, R.L., Vitousek, P.M., Reynolds, H.L., Hooper, D.U., Osvaldo, S.L., Sala, E., Hobbie, S.E., Mack, M.C. and Díaz, S.(2000). Consequences of Changing Biodiversity. *Nature* 405: 234–242.

Food and Agriculture Organisation (FAO). (2009). Sustaining Communities, Livestock and Wildlife: A Decision Support Tool. Project Implemented FAO-UN in collaboration with African Wildlife Foundation, ILRI and Government of Tanzania on a GEF/WB fund in Monduli and Simanjiro Districts, Northern Tanzania. Rome, Italy.

Flowers, B., Huang, K. and Aldana, G. O. (2020). Analysis of the Habitat Fragmentation of Ecosystem in Belize Using Landscape Metrics. *Journal of Sustainability MDPI* 2020 Vol. 12, 3024.

Giannini, T.C., Cordeiro G.D., Freitas B.M., Saraiva A.M., Imperatriz-Fonesca V.L., (2015). The Dependence of Crops for Pollinators and the Economic value of Pollination in Brazil

Hall S. (1977). Representation: Cultural Representations and Signifying Practices.

Huth, A. and Cebula, J., (2011). The Basics of Cloud Computing

Isichie A.O., Moughalu, J.I., Akeredolu F.A. and Afolabi, O.A. (1995). Fuel characteristic and Emission from Biomass Burning and land use change in Nigeria Environ Monitor.

Jensen, E. S., (1996). Grain yield symbiotic N_2 fixation and interspecific competition for inorganic N in pea-barley inter crops. Plant Soil 182, 25 – 38

Kumar Ashwini *and Briti Sundar Sil 2022: Impacts of Land Use and Land Cover Changes on Land Surface Temperature over Cachar Region, Northeast India—A Case Study *Journal of Sustainability, 14. 14807*

Lillesand, T. M. and Keifer, R. W., (2004). Remote Sensing and image interpretation fifth edition.

Lillesand, T. M. and Keifer, R. W. and Chipman, J. W., (2008). Remote Sensing and image interpretation sixth edition.

Lu, D. Mausel, P., Brondizo, E. and Moran, E. (2004) Change Detection Techniques. *International Journal of Remote Sensing*, Volume 25, 2004 – Issue 12.

Mandal, M and Chatterjee, N. D. (2020). Spatial alteration of fragmented forest landscape for improving structural quality of habitat: A case study from Radhanagar Forest Range, Bankura District, West Bengal, India. *Journal of Geology, Ecology and Landscapes.*

Meshach O. Aderele, Tomiyosi S. Bola, David O. Oke (2020), Land Use/Land Cover Changes of Ago-Owu Forest Reserve, Osun State, Nigeria Using Remote Sensing Techniques. *Open Journal of Forestry*, 10, 401-411 https://www.scirp.org/journal/ojf

Millenium Ecosystem Assessment (MEA). 2003. Ecosystems and Human-well Being: A Framework for Assessment. Island Press, Washington, D.C., USA.

Millennium Ecosystem Assessment (MEA). 2005. Ecosystems and Human Well-Being: synthesis. World Resources Institute, Washington, DC., USA.

Oates, H.I., Isichei, A.O. & Leonov S.E. 2014. Omo Biosphere Reserve, Current Status, Utilization of Biological Resources and Sustainable Management (Nigeria). Working Papers of the South South Cooperation Programme on XL-8, 2014. ISPRS Technical Commission VIII Symposium, 09-12 December, 2014, Hyderabad, India. pp. 613-616.

Ola Adams B.A. (1999). Biodiversity Inventory of Omo Biosphere Reserve, Nigeria – Country Report on Biosphere Reserves for Biodiversity Conservation and Sustainable Development, Abeokuta.

Oke, C.O. (2013). Terrestrial mollusc species richness and diversity in Omo Forest Reserve, Ogun State, Nigeria. *African Invertebrates* 54 (1): 93–104. [1

Parker, C. P., Baltes, B. B., Young, S. A., Huff, J. W., Altmann, R. A., LaCost, H. A. and Roberts J. E., (2003). Relationships between psychological climate perceptions and work outcomes: a meta-analytic review. J*ournal of organizational Behaviour*, Vol.24 Issue 4.

Rakesh Kumar, S. Nandy, Reshu Agarwal, S.P.S. Kushwaha, (2014). Forest cover dynamics analysis and prediction modeling using logistic regression model. Ecological Indicators (2014) 444–455

Slady Akike1, Sailesh Samanta, (2016). Land Use/Land Cover and Forest Canopy Density Monitoring of Wafi-Golpu Project Area, Papua New Guinea

Soraya Violini, (2013). Deforestation: Change Detection in Forest Cover using Remote Sensing.

Suhaili, A. B.; Helmi, Z. M.; Shafri, N. A. and Ainuddin, A. G. (2006). Improving Species Spectral Discrimination Using Derivatives Spectra For Mapping of Tropical Forest From Airborne Hyperspectral Imagery

Takayama, S. Bimston, D.N., Matsuzawa, S., Freeman, B.C., Aime-Sempe, C., Xie, Z., Morimoto, R.J. and Reed, J.C., (1997). Bag-1 modulates the chaperone activity of hsp70/hsc70 EMBO J 16 4887 – 4896.

United Nations Environment Programme (UNEP). (1992). Rio Declaration on Environment and development. http://www.unep.org/Documents.Multilingual/Default.asp? Document ID =78&ArticleID=1163. (25 Feb. 2012).

United Nations Environment Programme (UNEP). (2002). Global Environmental Outlook 3. Past, Present and Future Perspectives.

Uzoma D. C. and Moses O.A., (2014). Land Use Change Detection in OMO Biosphere Reserve Using GIS and Remote Sensing. *Journal of Environment and Ecology* ISSN 2157-6092 2014, Vol. 5, No. 2